Characterization of scatterers by their anisotropic and dispersive behavior

M. Duquenoy[†‡], J-P. Ovarlez[†], L. Ferro-Famil[‡], E. Pottier[‡] and L. Vignaud[†]

[†] : Signal Processing Unit, Electromagnetism and Radar Department (DEMR)
ONERA, Palaiseau, France
Chemin de la Hunière, F-91761 Palaiseau cedex
Telephone: (+33) 1 69 93 62 95, Fax: (+33) 1 69 93 62 69
Email : mickael.duquenoy@onera.fr

[‡] : Image and Remote Sensing Group, Institute of Electronics and Telecommunications from Rennes (IETR)
University of Rennes 1, Rennes, France
Campus Beaulieu, Bat 11D, 263 avenue Général Leclerc, CS-74205 Rennes cedex
Telephone: (+33) 2 23 23 67 14, Fax: (+33) 2 23 23 69 63
Email : laurent.ferro-famil@univ-rennes1.fr

I. Introduction

Synthetic Aperture Radar (SAR) images built from received signals are high-resolution maps of the spatial distribution of the reflectivity function of targets. Conventional radar imaging assumes that all the scatterers are considered as bright points (isotropic for all observation angles and white in the frequency band) [1]. Recent studies based on multidimensional Time-Frequency Analysis describe the angular and frequency behavior of scatterers and show that they are anisotropic and dispersive [2]. Another useful information source in radar imaging is the polarimetry. Studies based on multidimensional wavelet and coherent decompositions allow to represent the angular and frequency polarimetric behavior and show the non-stationarity of this behavior. The aim is to characterize scatterers by time-frequency analysis and polarimetry.

II. Highlighting the anisotropic and dispersive behavior of scatterers by two-dimensional time-frequency analysis

When a target is illuminated by a broad-band signal and/or for a large angular domain, it is realistic to consider that the amplitude spatial repartition $I(\vec{r})$ of the reflectors depends on frequency f and on the aspect angle θ. This repartition depending on the wave vector $\vec{k}$ will be noted in the following by $I(\vec{r},\vec{k})$. Such images can be built using the multidimensional continuous wavelet transform extended to two dimensions of the backscattering coefficient H and are called hyperimages [3]:

$$I(\vec{r_0},\vec{k_0}) = \int H(\vec{k})\,\Psi^*_{\vec{r_0},\vec{k_0}}(\vec{k})\,d\vec{k}\,. \tag{1}$$

where $\Psi_{\vec{r}_0,\vec{k}_0}(\vec{k})$ is a family of wavelet bases generated from the mother wavelet $\phi(k,\theta)$ localized around $(k,\theta) = (1,0)$ and located spatially at $\vec{r} = \vec{0}$ according to:

$$\Psi_{\vec{r}_0,\vec{k}_0}(\vec{k}) = \frac{1}{k_0}\,e^{-2i\pi\vec{k}.\vec{r}_0}\,\phi\left(\frac{k}{k_0},\theta-\theta_0\right). \tag{2}$$

In polarimetry, the scattering matrix or Sinclair matrix, will now depend on frequency and on the angle of presentation and is called hyper-scattering matrix :

$$[S](\vec{r},\vec{k}) = \begin{bmatrix} S_{hh}(\vec{r},\vec{k}) & S_{hv}(\vec{r},\vec{k}) \\ S_{vh}(\vec{r},\vec{k}) & S_{vv}(\vec{r},\vec{k}) \end{bmatrix} \tag{3}$$

The span is generally defined as the sum of the squared modulus of each element of the matrix. The extended span is now defined as the sum of the squared modulus of each element of the hyper-scattering matrix (3).

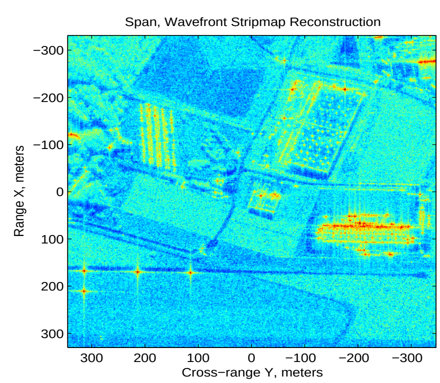

Fig. 1. Span of the image SAR.

$$\begin{aligned} Span(\vec{r},\vec{k}) &= |S_{hh}(\vec{r},\vec{k})|^2 + |S_{hv}(\vec{r},\vec{k})|^2 \\ &+ |S_{vh}(\vec{r},\vec{k})|^2 + |S_{vv}(\vec{r},\vec{k})|^2. \end{aligned} \tag{4}$$

The extended span is an energetic description of the anisotropic and dispersive behavior of scatterers. Let us rewritten $Span(\vec{r}, \vec{k})$, $Span(x; y; f; \theta)$: for each frequency f_o and each angle of radar illumination θ_o, $Span(x; y; fo; \theta o)$ represents a spatial repartition of reflectors which respond at this frequency and this angle. Inversely, for each reflector located at $ro = (xo; yo)$, we can extract its feature $Span(xo; yo; f; \theta)$ in frequency f and in angular θ. This is this aspect that we decided to point out in order to see if this quantity is anisotropic or/and dispersive.

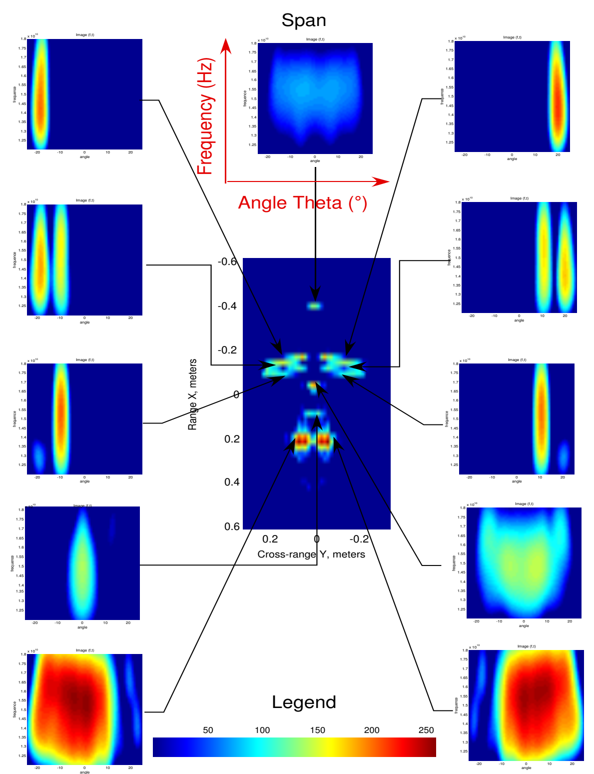

Fig. 2. Extended span of the weapon target Cyrano in anechoic chamber.

III. Study of the polarimetric stationnarity behavior by polarimetric hyperimages

The polarimetric behavior can be stationnary (ie. the polarimetric behavior is independent of the emitted frequency and the angular aspect) or non-stationnary (ie. the polarimetric behavior is dependent of the emitted frequency and the observation angle). The aim is to build a polarimetric representation versus the emitted frequency and the observation angle to characterize this behavior. In our case we are interested by man-made targets because they present a dispersive and anisotropic behavior. The basic tool to study the deterministic targets is the coherent decompositions [4], [5]. The objective of the coherent decompositions is to express the Sinclair matrix $[S]$ (ie. the measured scattering matrix by the radar) as a combination of the scattering responses of simpler objects:

$$[S] = \sum_{i=1}^{k} C_i [S]_i \tag{5}$$

By application of the coherent decompositions to the hyperscattering matrix we obtain representations of the polarimetric nature versus the emitted frequency and the observation angle. For example, the Cameron decomposition represents the Sinclair matrix $[S]$ as a combination of a maximum symetric component, a minimum symetric component and a nonreciprocal component. Indeed, it decomposes the scattering matrix according to :

$$\begin{aligned}\overrightarrow{S} = A \Big(\cos(\theta_{rec}) \Big(\cos(\tau)\, \overrightarrow{S}^{sym}_{max} + \sin(\tau)\, \overrightarrow{S}^{sym}_{min}\Big) \\ + \sin(\theta_{rec})\, \overrightarrow{S}_{nr}\Big)\end{aligned} \tag{6}$$

By application of the Cameron decomposition to the hyperscattering matrix, the following decomposition is obtained :

$$\begin{aligned}[S(\vec{r},\vec{k})] = A(\vec{r},\vec{k}) \Big\{\cos(\phi_{rec}(\vec{r},\vec{k})) \Big(\cos(\tau(\vec{r},\vec{k}))[S(\vec{r},\vec{k})]^{max}_{sym} \\ + \sin(\tau(\vec{r},\vec{k}))[S(\vec{r},\vec{k})]^{min}_{sym}\Big) + \sin(\phi_{rec}(\vec{r},\vec{k}))[S(\vec{r},\vec{k})]_{nr}\Big\}\end{aligned} \tag{7}$$

From the Cameron decomposition, a classification can be processed, see figure 3. This work leads to a new classification hyperimage $C(\vec{r}, \vec{k})$ and allows to extract the Huynen orientation $\psi(\vec{r}, \vec{k})$. For each $\vec{k_0}$, the classification hyperimage

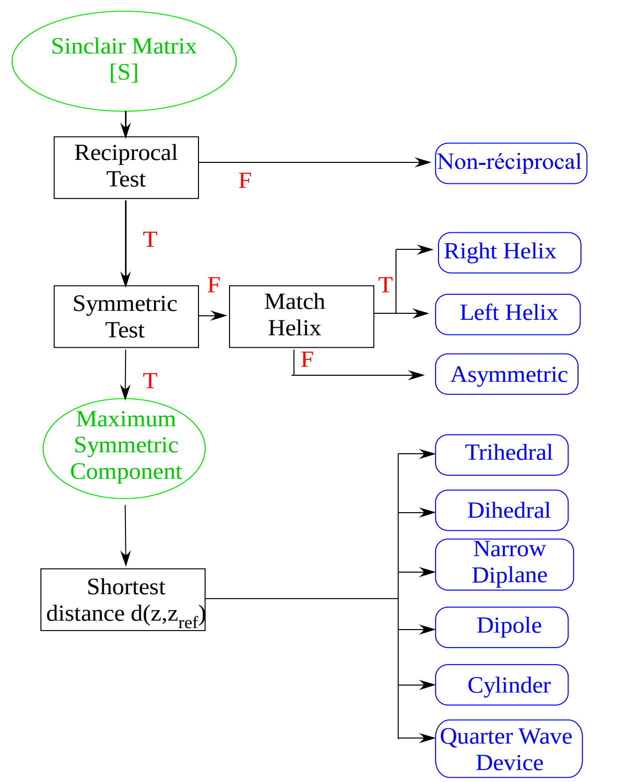

Fig. 3. Classification process of the Cameron decomposition.

and the Huynen orientation, represent the classification and the orientation of the target around the line of sight for an aspect angle and for an emitted frequency.

For each $\vec{r_0}$, the classification hyperimage and the Huynen orientation represent the polarimetric behavior evolution and the angle in the vertical plane of the scatterer located at $\vec{r_0}$.

These representations are called polarimetric hyperimages. Polarimetric hyperimages allow to describe the backscattering mechanisms by the orientations of scatterers and their nature. Studies based on polarimetric hyperimages showed the polarimetric behavior could be stationnary or non-stationnary [6]. In these cases the non-stationnary behavior is due to by the fact that the radar does not see the same geometry at different observation angles.

IV. Characteristics parameters of the polarimetric dispersive and anisotropic behavior

A scatterer can be isotropic or anisotropic, dispersive or non-dispersive, polarimetric behavior stationnary or non-stationnary. The goal is to extract characteristics parameters which highlight these three behaviors. The anisotropy and dispersivity can be expressed from the extended span. So, the marginal densities in the frequency and angular fields can be calculated.

$$Marginal_f(\overrightarrow{r}, f) = \frac{\int_\theta Span(\overrightarrow{r}, \overrightarrow{k})\, d\theta}{\int_\theta \int_f Span(\overrightarrow{r}, \overrightarrow{k})\, d\theta\, df} \tag{8}$$

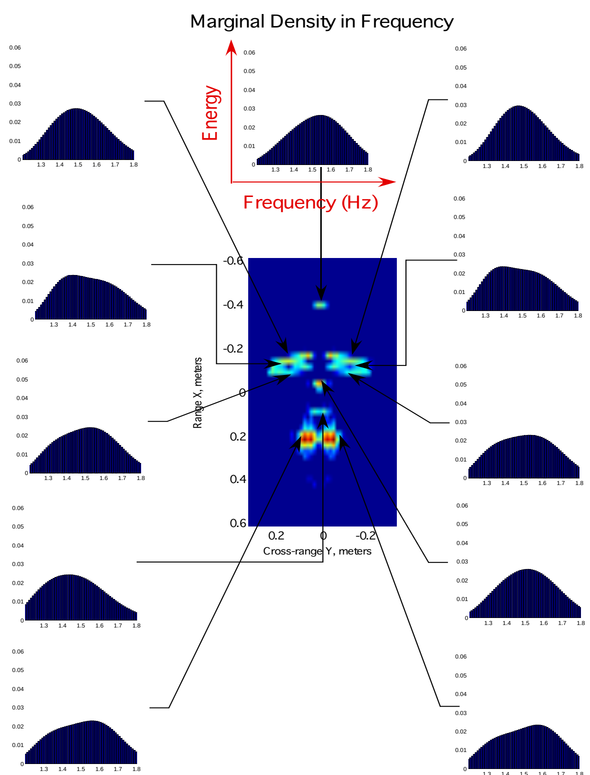

Fig. 4. Frequency marginal density of the weapon target Cyrano in anechoic chamber.

$$Marginal_\theta(\overrightarrow{r}, \theta) = \frac{\int_f Span(\overrightarrow{r}, \overrightarrow{k})\, df}{\int_\theta \int_f Span(\overrightarrow{r}, \overrightarrow{k})\, d\theta\, df} \tag{9}$$

From these densities the standard deviations are extracted. The standard deviation in frequency means the dispersivity, the standard deviation in angle means the anisotropy. Standards deviations have been tested on the SAR image of the figure 1. This image is composed of four calibrating trihedrals, three buildings and one parking. The standard deviation in frequency, figure 6, shows the buildings, trihedrals and parking have a strong value of the standard deviation. So, deterministics scatterers are non-dispersive, although natural media and vegetation have a low value of standard deviation and they can be considered as dispersive. The standard deviation in angle, figure 7, is not very meaning. These results can be explained by the fact that the angular excursion of the image is only two degrees. So we can not consider the angle information. Former

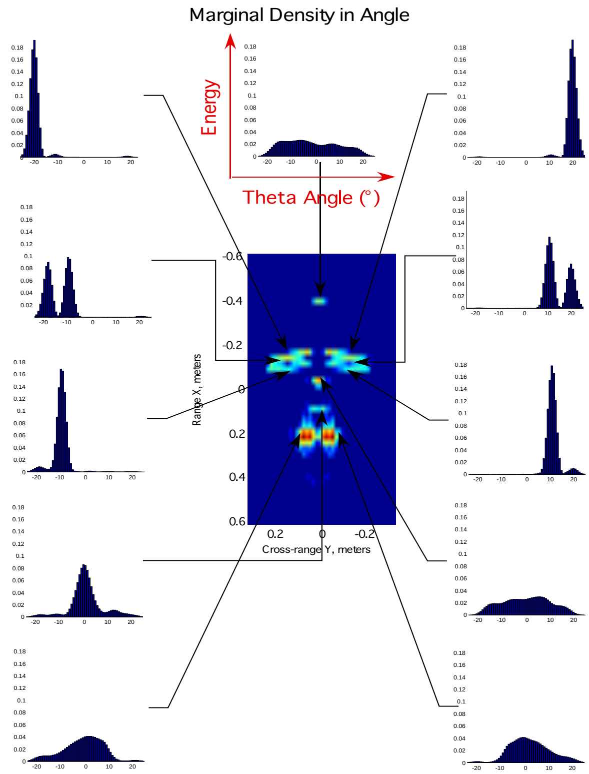

Fig. 5. Angular marginal density of the weapon target Cyrano in anechoic chamber.

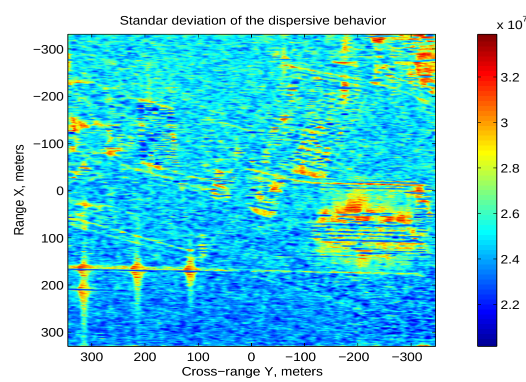

Fig. 6. Standard deviation of the frequency marginal density.

works show the anisotropy is important, for example on targets in anechoic chamber [7], however these former results are obtained for a angular excursion of fifty degrees.

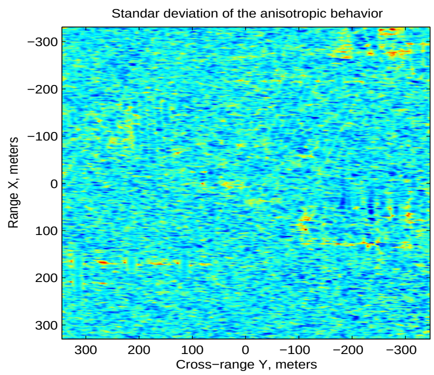

Fig. 7. Standard deviation of the angular marginal density

The polarimetric stationnary behavior can be expressed from the polarimetric hyperimage (noted $C(\overrightarrow{r}, \overrightarrow{k})$). Indeed, by using the Cameron decomposition as coherent decomposition, the polarimetric nature is given by a classification (Class). So, an energetic density of classification can be extracted.

$$D(\overrightarrow{r}, Class) = \frac{\int_f \int_\theta Span(\overrightarrow{r}, \overrightarrow{k}) \delta(C(\overrightarrow{r}, \overrightarrow{k}) - Class)\, d\theta\, df}{\int_\theta \int_f Span(\overrightarrow{r}, \overrightarrow{k})\, d\theta\, df} \tag{10}$$

So, if one class of the density is close to one the behavior is stationnary otherwise the behavior is non-stationnary. To classify scatterers into two classes, the polarimetric stationnary and non-stationnary scatterers, this parameter can be thresholded. The results on the image SAR, figure IV, show the trihedrals and some scatterers of buildings are stationnary. The limitations of this method are the using of a coherent method. Future work will propose the extraction of this parameter from the H/A/α decomposition.

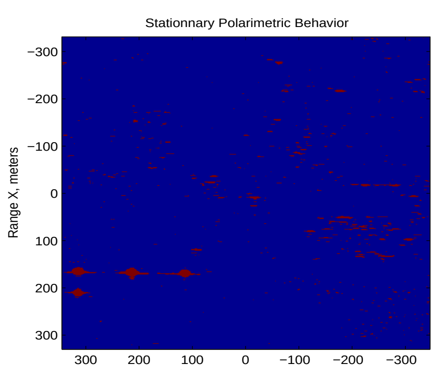

Fig. 8. Stationnary Polarimetric scatterer

V. Classification by the anisotropic and dispersive behavior of scatterers

From the standard deviations and the polarimetric density a classification can be processed. Indeed, the non-dispersive and dispersive scatterers can be separated by thresholding the standard deviation in frequency, the anisotropic and isotropic scatterers can be highlighted by thresholding the standard deviation in angle, and the stationnary or non-stationnary polarimetric behavior can be pointed out by thresholding the density. So, a classification into eight classes can be obtained.

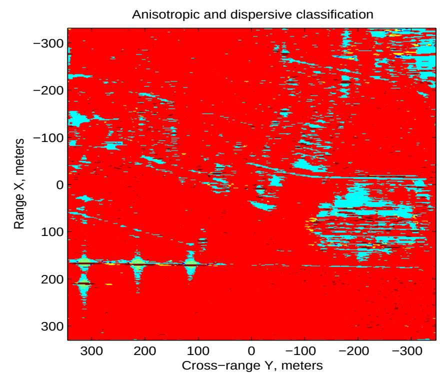

Fig. 9. Classification of the image SAR.

VI. Conclusion

A new method to characterize scatterers by their anisotropic and dispersive behavior is proposed. It highlights the fact that time-frequency analysis and polarimetry are well adapted to characterize scatterers. Future work will consist in finding parameters more pertinent and in developping other classification algorithm.

References

[1] D.L. Mensa, *High Resolution Radar Imaging*, Artech House, USA, 1981.

[2] M. Duquenoy, J.P. Ovarlez, L. Vignaud, L. Ferro-Famil, E. Pottier, *SAR Imaging Using Time-Frequency Analysis*, Proc PSIP conference, 31 jan-02 feb 2007, Mulhouse, France.

[3] J.P. Ovarlez, L. Vignaud, J.C. Castelli, M. Tria and M. Benidir, *Analysis of SAR Images by Multidimensional Wavelet Transform*, IEE-Radar, Sonar and Navigation, Special issue on time-frequency analysis for synthetic aperture radar and feature extraction, 150(4), august 2003, 234-241.

[4] E. Krogager, Z. H. Czyz, *Properties of the Sphere, Diplane, Helix Decomposition, Proceeding of the Third International Workshop on Radar Polarimetry, Nantes, Mar. 1995.*

[5] W. L. Cameron, N. N. Youssef and L. K. Leung, Simulated Polarimetric Signatures of Primitive Geometrical Shapes*, Trans. IEEE Geosci. Remote Sensing, 34(3), may 1996, 793-803.*

[6] M. Duquenoy, J.P. Ovarlez, L. Ferro-Famil, L. Vignaud and E. Pottier, Study of Dispersive and Anisotropic Scatterers Behavior in Radar Imaging Using Time-Frequency Analysis and Polarimetric Coherent Decompositions.*, Proc. EUSAR conference, 16-18 may 2006, Dresden, Germany.*

[7] M. Duquenoy, J.P. Ovarlez, L. Ferro-Famil, L. Vignaud and E. Pottier, Study of Dispersive and Anisotropic Scatterers Behavior in Radar Imaging Using Time-Frequency Analysis and Polarimetric Coherent Decompositions.*, Proc. IEEE International radar conference, 24-27 april 2006, Verona, NY, USA.*